Autonomous recovery of a Fixed-wing UAV Using a Line Suspended Between Two Multirotor UAVs

Mads Friis Bornebusch*, Tor Arne Johansen*
*Centre for Autonomous Marine Operations and Systems (AMOS), Department of Engineering Cybernetics, Norwegian University of Science and Technology, Trondheim, 7491, Norway

***Abstract*—This article presents an autonomous recovery system for fixed wing UAVs which is using a line suspended between two multirotor UAVs to catch a line with a hook hanging from a fixed-wing UAV. This method of recovery is particularly suitable for recovery in space constrained areas such as on small ships. A control system is presented for the proposed recovery concept and the concept is validated through experiments. The results include 17 test runs to characterize control accuracy, followed by 3 successful recoveries. With the selected equipment and tuning values, the multirotors were able to track the fixed-wing UAV with a mean error of 0.8 m at the moment the catch would have happened in the 17 test runs. The margins for missing for the three recoveries were 1.0-2.1 m showing that this recovery method is robust.**

I. Introduction

A. Motivation and main idea

Fixed-wing UAVs are used for a wide range of missions such as surveying and monitoring. Compared to multirotor UAVs they have a longer range and endurance. One main advantage of multirotor UAVs over the fixed-wing type is the ability to take off and land vertically. This capability offers a great deal of operational flexibility. Using a catapult with springs, rubber bands or pneumatics for launching the fixed-wing UAV can provide some of the same operational flexibility for the fixed-wing UAV platform. However, the problem of recovery of fixed-wing UAVs, and in particular autonomous recovery, still stands and has been covered extensively by the research literature as summed up in [1].

In this paper we propose a concept for autonomous recovery of a fixed wing UAV by using a line suspended between two multirotors and a line with a hook hanging from the fixed-wing UAV. The line on the fixed-wing UAV is connected to a single hard point close to the center of gravity of the plane which can absorb the impact without damage to the equipment.

B. Literature review

If a fixed-wing airframe capable of vertical takeoff and landing (VTOL) is used, it can be landed automatically by using techniques similar to landing multirotor UAVs. With tilted rotors or a set of dedicated rotors for the vertical motion mode, the control system must handle both modes as well as the transition, [2]. Hybrid VTOL fixed-wing UAVs are usually specifically designed to have this capability, something which requires compromises to be made on e.g. range or payload capacity, [3], [4]. Hence, it is not always possible to add VTOL capabilities to a regular fixed-wing platform, and the VTOL capability comes with some penalties such as increased weight, drag and complexity of the system.

In order to land fixed-wing UAVs automatically, vision based systems have been developed such as in [5] and [6] where automatic landing of fixed-wing UAVs on a conventional runway is achieved. Vision based systems have also been used for landing fixed-wing UAVs using various arrest mechanisms other than a runway such as in [7] where a fixed-wing UAV is landed in a net, in [8] where an airbag is used, and in [9] where a fixed-wing UAV is landed on a car-top. Other systems are using high precision GNSS systems for landing fixed-wing UAVs such as in [10] where a fixed-wing UAV is recovered in a net using a real time kinematic (RTK) global navigation satellite system (GNSS). Another way of landing UAVs is with a high angle of attack in a so called deep stall. In [11] a simulation study is presented for a system capable of precision landing a fixed-wing UAV in a deep stall.

One unconventional landing system that is not much studied in the scientific literature is the concept used for recovery by the company Zipline [12]. This concept uses a rod with a hook under a fixed-wing UAV in order to catch a horizontal line suspended between two poles and a big mattress to soften the landing. Another system is the SkyHook by Insitu which uses a crane to suspend a vertical line and a hook at the wing tip of the UAV to catch the line [13]. DARPA is prototyping a concept where a hook on top of the UAV catches a horizontal line suspended on a rail [14], and towed cable systems have been studied for rendezvous of small UAVs [15]. The concept of using two multirotors to cooperatively carry a net used to recover a fixed-wing UAV in the air was first described in [16] and was later verified by experiments in [17]. However, this concept has some drawbacks as the net adds extra weight and increases the sensitivity to wind. To limit these disadvantages a smaller net can be used, but that will lead to a higher precision requirement for the coordination between the multirotors and fixed-wing UAV. During the impact between the fixed-wing UAV and the net there is a risk of damage to fragile equipment mounted on the fixed wing UAV such as the pitot-tube, propeller, antennas, cameras and other sensors.

C. Contributions

The drawbacks of the concept in [17] are addressed in this article where an improved concept is presented and verified by experiments. The main contribution is the design of a system

that demonstrates through flight experiments the feasibility of a concept for autonomous recovery of a fixed wing UAV by using a line suspended between two multirotors and another line with a hook hanging from the fixed-wing UAV. The main contribution of this article is the control system design.

D. Organization

The article is organized as follows. In Section II the concept and its advantages are described, and important definitions are given. Section III is describing the controllers, control structure and algorithms. In Section IV the experimental platform and operational aspects are described, and in Section V the results from the experiments are presented and analysed. The article is concluded by Section VI and Section VII with a discussion of future improvements and concluding remarks.

II. Line-catch Concept

The concept of fixed-wing UAV recovery described in this paper uses a line suspended between two multirotor UAVs. This line will be referred to as the multirotor line. In order to get the fixed-wing UAV attached to the multirotor line, another line is released from a pod attached to the fixed-wing UAV before the catch. This line will be referred to as the catch line. The catch line has a weight and a hook at the end with the purpose of weighing the line down and catching the multirotor line respectively. A sketch of this system is shown in Figure 1(a). The multirotor line is slack and hanging below the multirotors to avoid the risk of getting this line tangled up in the rotors of the multiorotors. In order for the catch to happen, the fixed-wing UAV passes under and in-between the multirotors such that the catch line intercepts the multirotor line. It is beneficial to let the fixed-wing UAV pass below the multirotors to avoid the catch line hanging from the plane getting tangled in the rotors of the multirotors. When the fixed-wing UAV passes the multirotors, the hook at the end of the catch line will intercept the multirotor line, and the fixed-wing is thereby caught. After the catch, the fixed-wing hangs below the multirotors as seen in Figure 1(b) and can be lowered to a specific location for a successful recovery.

The line-catch concept is designed for recovery of fixed wing UAVs where there is a constraint on space which makes it impossible to land a fixed-wing UAV in the conventional way, for example on a small ship. By recovering the fixed wing with a line-catch, the recovery can be moved away from the ship which will give a number of advantages:

- **Little interference with other operations** as the system only needs a small space to be cleared for takeoff and landing of the multirotors.
- **Not much affected by waves, wind and turbulence** as there is only low wind drag in the thin lines used for recovery, and the course of the fixed-wing UAV can be aligned to be against the mean wind direction.
- **Low risk to personnel** as the fixed wing UAV does not need to fly close to the ship.
- **Small impact force** on the fixed-wing UAV as the relative velocity between the multirotors and the fixed-wing UAV can be controlled to be lower than the ground speed of the fixed-wing UAV. This impact force can be tuned by the multirotor position controller gains, that can be designed using a spring/damper analogy.
- **Few structural requirements to the airframe of the fixed-wing UAV** as it only needs to have a small pod containing the catch line mounted on the belly.

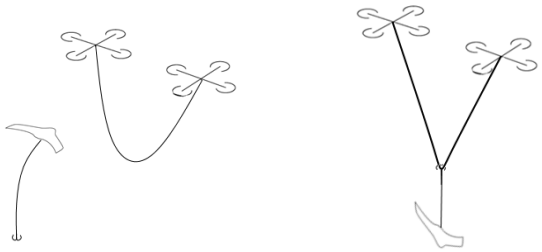

(a) Before catch (b) After catch

Fig. 1: Illustration of the line-catch concept just before and after the catch.

A. Line-catch maneuver

The line-catch maneuver starts when the recovery is initiated and ends when the fixed-wing UAV has been caught. During the maneuver, the fixed-wing UAV will fly a straight path at constant altitude. The coordination required to position the vehicles such that the fixed-wing UAV is caught is done autonomously by the multirotors as they are the more agile platform. The line-catch maneuver is therefore carried out by the multirotors, while the fixed-wing UAV follows a pre-planned straight path called the virtual runway.

B. Virtual runway, reference frames and notation

The area where the line-catch maneuver takes place will be referred to as the virtual runway, as illustrated in Figure 2. The virtual runway is defined by a center line of length l_{rwy}. The line-catch maneuver is set up such that the center line of the virtual runway coincides with the planneded path of the fixed-wing UAV.

The following reference frames are defined first:

- Local north-east-down (NED) frame, $\{n\}$, assumed inertial.
- Path frame, $\{p\}$, which has its origin at the start of the virtual runway, as further illustrated in Figure 3. Its x axis is pointing along the virtual runway, its z axis points down, and the y axis completes the right hand system.
- Formation centroid frame, $\{c\}$. Origin at an offset, z_{off}, below the middle of the multirotor formation. The z-axis is aligned with the z-axis of $\{n\}$ and the yz-plane is defined as having both multirotors in it. It can be described as the body-frame for the multirotor formation.

Vector positions will be described with $\boldsymbol{p}_k^b$, velocities with $\boldsymbol{v}_k^b$, and accelerations with $\boldsymbol{a}_k^b$. Trailing superscripts b is the reference frame, trailing subscripts k are identifiers:

- fw: Fixed-wing UAV
- c: Centroid of multirotor formation

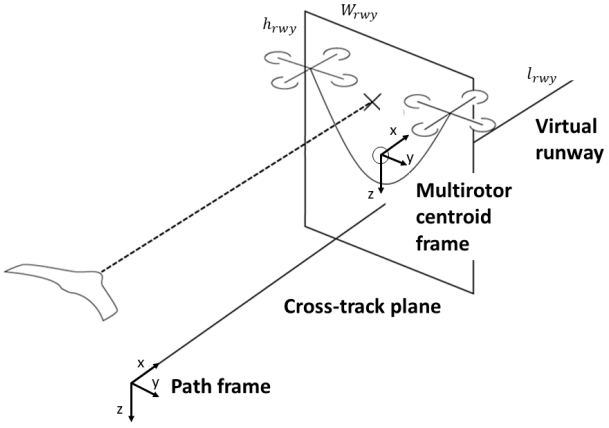

Fig. 2: Illustration of the virtual runway. Its defining line starts at the origin of the path frame, and it has a defined length ℓ_{rwy}. The origin of the multirotor formation centroid frame is symbolized with a circle. The cross-track plane is defined by the yz-axes of this frame, and the virtual runway is limited laterally by its width W_{rwy} and vertically by its height h_{rwy}.

- d: Desired path (reference)
- l: Left multirotor as seen from the fixed-wing UAV before recovery
- r: Right multirotor as seen from the fixed-wing UAV before recovery

Subscripts 1,2,3 refers to elements of the vector. Multiplication of a vector with the matrix $\boldsymbol{R}_a^b$ rotates the vector from the reference frame a to the reference frame b. Additional notation is introduced subsequently, and the key parameters are summarized in Table II for easy reference.

The centroid of the formation is positioned relative to the virtual runway with an along track distance with coordiante $p_{c,1}^p$, and a cross track plane with coordinates $(p_{c,2}^p, p_{c,3}^p)$.

C. Maneuver stages

The line-catch maneuver is made up of different stages where the behaviour of the multirotors is different. In the first stage the multirotors are at the start of the virtual runway waiting for the fixed-wing UAV to approach. When the fixed wing UAV approaches, the second stage starts, and the multirotors will start the coordination with the fixed-wing UAV. The third stage is after the catch is detected where the multirotors will brake to a standstill and the maneuver ends. These three main stages are further subdivided into states, which will be explained in section III-A.

III. Control Design

Control of the fixed-wing UAV is carried out by a standard autopilot. The control structure for the multirotors is shown in Figure 4 and is based on the control structure in [17]. All the variables in Figure 4 are updated autonomously onboard the UAVs in-flight. The prescribed parameters that define the overall behavior of the system will be introduced in this

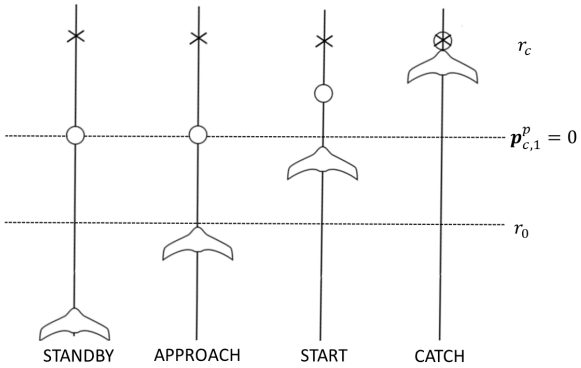

Fig. 3: Along track coordination. The centroid of the multirotor formation is symbolized with a circle. The desired point of recovery is a cross. The multirotors are in STANBY and APPROACH states at the start of the virtual runway, $p_{c,1}^p = 0$. When the fixed-wing UAV reaches the distance r_0 from the start of the virtual runway the START state is entered, and the multirotor formation will start the along track coordination and thus move along the virtual runway with the desired speed.

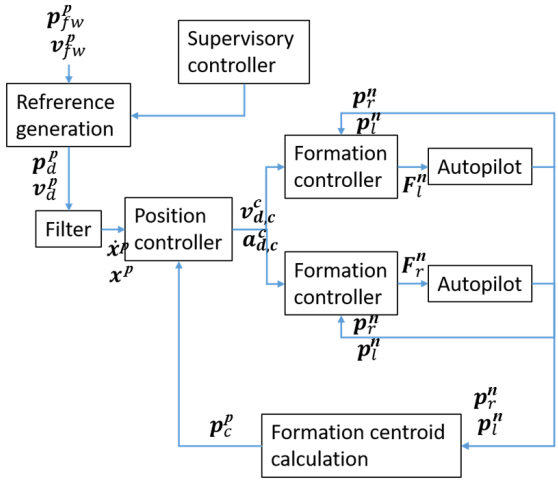

Fig. 4: Block diagram of the structure of the controller

section, and are later summarized in a table. Low level control of each multirotor is carried out by an autopilot which takes a commanded force in NED coordinates that should be applied as input. The autopilot will control the attitude and the total thrust of the propellers such that this force is achieved.

The formation control of the multirotors is carried out by a controller which is given a desired formation centroid velocity $\dot{\mathbf{x}}^p$ and a desired formation centroid position $\mathbf{x}^p$. Each of the multirotors will synchronize their relative position in order to maintain the desired formation and motion. Position and velocity measurements are shared between the vehicles.

This section will cover the control design for the coordination of the multirotor formation and the fixed-wing UAV in order to catch the fixed-wing UAV. This consists of a supervisory controller, reference generation, a reference filter and a position controller. The state of the supervisory controller decides which references are used.

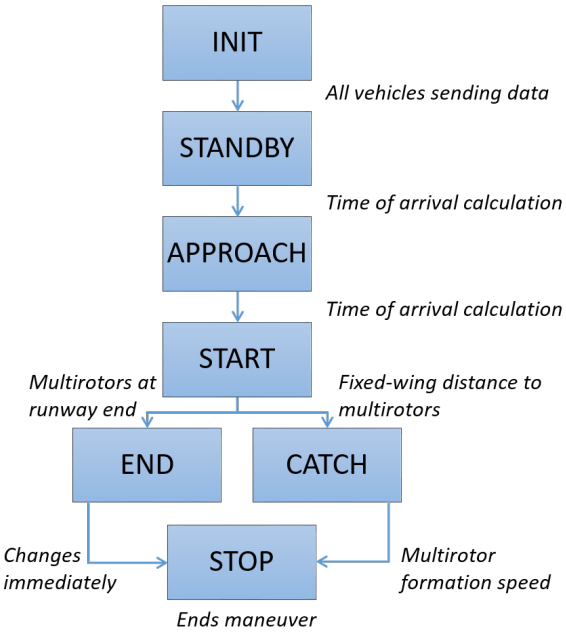

Fig. 5: State machine for the supervisory controller

A. Supervisory control

The supervisory control is similarto [16] and is responsible for changing between the different states in the three stages of the line-catch. The states are listed in Table I along with the corresponding behaviour of the multirotors. Figure 5 is showing the state machine which implements the state change logic. The first stage of the line-catch consists of the INIT and STANDBY states where the multirotors hold the position at the start of the virtual runway. The second stage involves the states APPROACH and START where the multirotors are tracking the fixed-wing UAV in order to catch it. In the APPROACH state, the multirotors track the fixed wing UAV position and velocity in the cross track plane while staying at the start of the virtual runway. In the START state, the multirotors track the fixed-wing UAV in the cross track plane, and follows a reference velocity in the along-track direction. This will be described more in detail in Section III-C. The final stages of a successful maneuver are CATCH and STOP where the fixed-wing UAV turns off its propulsion, and the multirotors brake and end the maneuver. If no catch is detected, the fixed-wing UAV will turn on propulsion again, and the multirotors will go to the END stage when they are at the end of the virtual runway and then to STOP. The ABORT state is entered if an automatic abort is triggered, this is covered in Section IV-C. This state is not shown in Figure 5 as it can be entered from any of the other states.

B. State change logic

The conditions for changing between the states are shown in Figure 5. They are simplified version of the actual conditions which will be described below.

1) STANDBY: The condition for leaving STANDBY and starting the line-catch maneuver is based on a time of arrival type calculation of when the multirotors need to start the along-track coordination in order to catch the fixed-wing UAV at $r_c = 0.75 l_{rwy}$, which is the planned catch point along the virtual runway center line (in the $\{p\}$ coordinate frame). The calculation is based on an along track velocity profile of the multirotors of constant acceleration until a desired speed is reached, and then constant speed after that. The fixed-wing UAV's position along the cirtual runway where the multirotors need to start the along-track coordination is:

$$r_0 = v_{fw}\left(\frac{v_{ref}}{a_{ref}} + \frac{1}{v_{ref}}\left(r_c - \frac{v_{ref}^2}{2a_{ref}}\right)\right) - r_c \tag{1}$$

where v_{ref} and a_{ref} is the desired speed and acceleration of the multirotors respectively and v_{fw} is the ground speed of the fixed wing UAV. The first term in the parenthesis is the time it takes for the multirotors to reach v_{ref} from a standstill and the second term is the time it takes them to travel the remaining distance to r_c. The first term of the equation is therefore the distance travelled by the fixed-wing UAV while the multirotors move to r_c. The multirotor speed and acceleration need to be such that $r_0 > 0$. The condition for this is found as:

$$\lim_{a_{ref}\to\infty} r_0 = r_c\left(\frac{v_{fw}}{v_{ref}} - 1\right) \tag{2}$$

which gives us $v_{fw} > v_{ref}$ to have $r_0 > 0$. This means that the fixed-wing UAV needs to have a higher ground speed than the reference speed of the multirotors. In order to ensure that the line/hook-arrangement works and to avoid too high tension, one wants to ensure that a suitable nominal relative speed $v_{rel}^* > 0$ is achieved by choosing $v_{ref} = v_{fw} - v_{rel}^*$. There are constraints on the maximum speed and acceleration of the multirotors that must also be considered, and the wind speed and direction must be accounted for since both v_{ref} and v_{fw} are referenced with respect to the ground.

The conditions for changing out of the STANDBY state and thereby starting the line-catch maneuver are:

$$|\boldsymbol{p}_{fw,1}^p| < 1.5 r_0 \tag{3}$$

$$|\boldsymbol{p}_{fw,2}^p| < \frac{w_{rwy}}{2} \tag{4}$$

$$|\boldsymbol{p}_{fw,3}^p| < \frac{h_{rwy}}{2} \tag{5}$$

$$|\boldsymbol{v}_{fw,2}^p| < v_{side} \tag{6}$$

where w_{rwy} is the width of the virtual runway, h_{rwy} is the height of the virtual runway and v_{side} is the maximum allowed velocity of the fixed-wing UAV in the lateral direction of the cross track plane. When these conditions are met, the state will change to APPROACH. The first condition is on the distance between the fixed-wing UAV and the start of the virtual runway. The second and third condition is that the position of the fixed-wing UAV in the cross track plane needs to be inside the virtual runway bounding box. The last condition is that the velocity of the fixed-wing UAV in the lateral (y) direction of the cross track plane should be less than some constant. In general, if these parameters are too large there is a risk that the fixed-wing UAV might be too far away from the virtual runway, and that the recovery will be unsuccessful and must be aborted. If they are too small, there

TABLE I: Line-catch states and behaviours

State	Behaviour
INIT	Checks if data is received from all vehicles
STANDBY	Multirotors holds position at start of virtual runway
APPROACH	Multirotors are tracking the fixed-wing in the cross-track plane of the virtual runway
START	Same as APPROACH but multirotors now also do along-track coordination
CATCH	Multirotors brake slowly until the formation velocity is zero
END	Signals that multirotors reached end of runway and failed the catch
STOP	Signals end of the maneuver
ABORT	Ends the manuever and starts the ABORT maneuver

is a risk that the fixed-wing UAV might have to go around for another attempt. They should therefore be tuned based on the dynamics of the fixed-wing UAV and the margins of the recovery system.

2) APPROACH: The condition for changing is that the fixed-wing UAV is at the distance where the multirotors need to start following the along track reference:

$$\boldsymbol{p}^p_{fw,1} < r_0. \tag{7}$$

When this condition is met, the state will change to START.

3) START: The catch itself is detected based on the fixed-wing distance to the planned catch point. Using the distance to detect the catch instead of e.g. force sensors on the multirotor line gives the advantage that the navigation and control system can be tested and tuned without any lines before a catch is attempted. The condition for changing to the CATCH state is:

$$||\boldsymbol{p}^p_{fw} - \boldsymbol{p}^p_c|| \leq r_{catch} \tag{8}$$

where r_{catch} is catch detection distance. If the multirotors reach the end of the runway without detecting a catch, they will go into the END state instead. The condition for this is:

$$\boldsymbol{p}^p_{c,1} > l_{rwy}. \tag{9}$$

4) CATCH: The condition for changing out of this stage is that the multirotors have come to a standstill:

$$||\boldsymbol{v}^p_c|| \leq v_{stop} \tag{10}$$

where v_{stop} is the velocity where the multirotors can be regarded as being at a standstill. When this condition is met the state will change to STOP. With this condition, the state change logic is not able to detect a missed catch. In order to detect this, the weight measurements from the load cells should be taken into account as well with the following condition:

$$W_{sum} \geq m_{thr} \tag{11}$$

where W_{sum} is the sum of the weight measurements from the two drones and m_{thr} is the weight threshold for when a catch is detected. An alternative is to monitor the fixed-wing UAV's speed or position relative to the multirotors.

C. Reference generation of formation centroid

In the STANDBY state the multirotors are holding a position at the start of the runway. The reference of the formation centroid is therefore zero both for the velocity and the position:

$$\boldsymbol{p}^p_d = \boldsymbol{0} \tag{12}$$

$$\boldsymbol{v}^p_d = \boldsymbol{0}. \tag{13}$$

In the APPROACH state the multirotors are tracking the fixed-wing UAV in the cross track plane, while still being at zero position in the along-track direction with respect to the path reference frame. The references are therefore:

$$\boldsymbol{p}^p_d = \begin{bmatrix} 0, \boldsymbol{p}^p_{fw,2}, \boldsymbol{p}^p_{fw,3} \end{bmatrix}^\top \tag{14}$$

$$\boldsymbol{v}^p_d = \begin{bmatrix} 0, \boldsymbol{v}^p_{fw,2}, \boldsymbol{v}^p_{fw,3} \end{bmatrix}^\top. \tag{15}$$

In the START state the multirotors start following the along track velocity profile while still tracking the fixed-wing UAV in the cross track plane. The reference for the formation centroid is:

$$\boldsymbol{p}^p_d = \begin{bmatrix} \boldsymbol{x}^p_1, \boldsymbol{p}^p_{fw,2}, \boldsymbol{p}^p_{fw,3} \end{bmatrix}^\top \tag{16}$$

$$\boldsymbol{v}^p_d = \begin{bmatrix} v^p_{d,x}, \boldsymbol{v}^p_{fw,2}, \boldsymbol{v}^p_{fw,3} \end{bmatrix}^\top \tag{17}$$

with $\boldsymbol{x}^p_1$ being the along-track coordiante of the filtered along-track position in (19)-(21) and with the along track velocity profile given by:

$$v^p_{d,x} = \min((t - t_0)a_{ref}, v_{ref}) \tag{18}$$

where t_0 is the time when the START state is entered.

D. Reference filter

The references are filtered in order to generate smooth signals for the formation centroid controller. The filter is a third-order filter based on [17]:

$$\boldsymbol{\tau}_1 = \text{sat}(k_1(\boldsymbol{p}^p_d - \boldsymbol{x}^p), v_{max}) \tag{19}$$

$$\boldsymbol{\tau}_2 = \text{sat}(k_2(\boldsymbol{\tau}_1 + \boldsymbol{v}^p_d - \dot{\boldsymbol{x}}^p), a_{max}) \tag{20}$$

$$\ddot{\boldsymbol{x}}^p = k_3(\boldsymbol{\tau}_2 - \ddot{\boldsymbol{x}}^p) \tag{21}$$

with the gains

$$k_3 = (2\zeta + 1)\omega_0 \tag{22}$$

$$k_2 = \frac{(2\zeta + 1)\omega_0^2}{k_3} \tag{23}$$

$$k_1 = \frac{\omega_0^3}{k_3 k_2} \tag{24}$$

where ω_0 and ζ are tuning parameters of the filter. The input to the reference filter is the desired velocity, $\boldsymbol{v}^p_d$, which comes from the reference generator. The output of the filter is the filtered position $\boldsymbol{x}$, velocity $\dot{\boldsymbol{x}}^p$ and acceleration $\ddot{\boldsymbol{x}}^p$ with respect to the path frame. The parameters v_{max} and a_{max} are the maximum desired speed and acceleration of formation

centroid. They should be chosen based on the dynamics of the multirotor UAVs and accounting for the along track wind speed since the centroid reference is with respect to the ground.

E. Formation centroid position control

The position controller is a PI-controller with velocity feed-forward:

$$\boldsymbol{v}_{d,c}^{p} = \dot{\boldsymbol{x}}^{p} + \boldsymbol{K}_{p}(\boldsymbol{x}^{p} - \boldsymbol{p}_{c}^{p}) + \boldsymbol{K}_{i}\int_{0}^{t}(\boldsymbol{x}^{p} - \boldsymbol{p}_{c}^{p})\mathrm{d}t \tag{25}$$

where $\boldsymbol{K}_p$ and $\boldsymbol{K}_i$ are diagonal gain matrices. The acceleration output from the filter is also used as a feed-forward to the formation controller:

$$\boldsymbol{a}_{d,c}^{p} = \ddot{\boldsymbol{x}}^{p}. \tag{26}$$

The control signals sent to the multirotors formation controller are transformed from the path frame p to the formation centroid frame c using the rotation matrix $\boldsymbol{R}_{p}^{c}$:

$$\boldsymbol{v}_{d,c}^{c} = \boldsymbol{R}_{p}^{c}\boldsymbol{v}_{d,c}^{p} \tag{27}$$

$$\boldsymbol{a}_{d,c}^{c} = \boldsymbol{R}_{p}^{c}\boldsymbol{a}_{d,c}^{p} \tag{28}$$

F. Multirotor formation control

The formation control of each multirotor is based on the following model, [18]:

$$m\dot{\boldsymbol{v}}_{*}^{n} = m\boldsymbol{g}^{n} + \boldsymbol{F}_{*}^{n} + \tau_{L}^{n} \tag{29}$$

where m is the mass of the multirotor, $\boldsymbol{g}^n$ is the gravitational acceleration vector $[0, 0, g]^\top$, $\boldsymbol{F}_{*}^{n}$ is the control force and τ_{L}^{n} is the disturbance from wind, and $*$ is a placeholder for the left (l) and right (r) multi-rotors. All quantities are given in the NED frame, $\{n\}$. This force control input is used on each multirotor in a passivity based formation controller based on [19]. This controller takes a desired formation velocity, $\boldsymbol{v}_{d,c}^{c}$, and acceleration, $\boldsymbol{a}_{d,c}^{c}$, as the input, and calculates the required control force, $\boldsymbol{F}_{*}^{n}$, for each multirotor UAV while an adaptive loop estimates and compensates for the disturbance force τ_{L}^{n}. The details of this controller are given in [20].

IV. Experimental validation

The experiments were carried out over two days in November of 2018 at Eggemoen UAV test centre in Norway. The winds were calm at 1-2 m/s from north on the first day and 1-2 m/s from north, northeast and east on the second day. Test runs were carried out before doing the actual catches to train the operational procedures and verify that a catch was possible.

The experimental validation of the concept was carried out using relatively small and low cost airframes. The values of the different parameters used for the experiments are shown in Table II.

A. System architecture

The system architecture for the multirotors and fixed-wing UAV form is very similar to that in [17] as the same hardware platforms have been used for these experiments.

Both multirotors are equipped with an autopilot, a companion computer (CC), a 5.8 GHz network radio link and a GNSS receiver on board. Due to space and weight constraints in the fixed-wing UAV platform it only has an autopilot, GNSS receiver and a radio link. The raw GNSS pseudo-range and carrier-phase measurements from the fixed-wing UAV's GNSS receiver are sent over a 2.4 GHz radio link to a companion computer on the ground. The fixed-wing UAV is controlled by ArduPlane running on the Pixhawk autopilot in the airframe. The autopilot in the fixed-wing UAV is responsible for both low level control and high level guidance. The details of the components of the fixed-wing system are given in Table III.

The multirotors have a Pixhawk autopilot running a custom version of APM:Copter. The APM:Copter software is customized such that the control input to the autopilot is a desired force or acceleration. Details of this customization are given in [17]. The formation controller, the position controller and the supervisory controller are all running on the CC and are implemented in DUNE which is a modular software framework that is part of the LSTS toolchain, [21]. The CC receives raw GNSS pseudo-range and carrier-phase measurements from the GNSS receiver and from a base station. This data is used by the open source library RTKLIB to calculate a RTK-GNSS position with centimeter level position accuracy [22]. The specifications of the components of the multorotor UAVs are shown in Table IV, and are further described in [23].

The operator interface is a laptop computer running Neptus which is the ground control segment from the LSTS toolchain. An overview of the system architecture is given in Figure 6.

B. Catch hardware

A quick-release mechanism is attached to the bottom of the multirotors for holding and releasing the multirotor line. The quick-release mechanism also consists of a tension sensor to measure the forces from the line. The multirotor line is a 19 m long 5 mm nylon flag rope capable of lifting 50 kg. This line is vastly over dimensioned but the thickness proved an advantage as it was easy to see in the air.

The catch line is a 5 m long 0.5 mm kevlar string. At the end of the line a 12.5 g lead weight is mounted. Approximately 10 cm above the end of the line, a hook is mounted. The hook is a treble fishing hook where the points have been filed blunt. The catch line, weight and hook are kept in a 3D printed pod under the fixed-wing UAV, which was developed in [24]. The pod, shown in Figure 7, is mounted on the fixed-wing airframe using fibre reinforced tape and can be opened by a remote controller.

C. Emergency and Abort behaviour

In order to ensure the safety of the operation, an abort maneuver can be triggered in case of abnormal behaviour or an emergency situation. The following conditions will trigger an abort:

TABLE II: Parameter values

Symbol	Value	Description
l_{rwy}	$57.7\ m$	Virtual runway length
w_{rwy}	$40\ m$	Virtual runway width
h_{rwy}	$20\ m$	Virtual runway height
l_{ml}	$19\ m$	Multirotor line length
l_{cl}	$5\ m$	Catch line length
v_{ref}	$5\ m/s$	Multirotor along-track velocity
a_{ref}	$5\ m/s^2$	Multirotor along-track acceleration
r_c	$0.75\ l_{rwy}$	Desired along-track catch point
v_{side}	$3\ m/s$	Maximum sideways velocity for the fixed-wing
r_{catch}	$2.5\ m$	Distance between fixed-wing and multirotor formation to detect catch
v_{stop}	$0.5\ m/s$	Multirotor stop detection max velocity
z_{off}	$3\ m$	Formation middle to $\{c\}$ (centroid) offset.
ζ	$1.15, 1.1$	Filter damping in normal conditions and in APPROACH/START state
ω_0	$0.5, 0.9$	Filter natural freq. in normal conditions and in APPROACH/START state
$\boldsymbol{K}_p$	$0.5\ \mathrm{diag}(1,1,1)$	Position control proportional gains
$\boldsymbol{K}_i$	$\mathrm{diag}(0,0,0)$	Position control integral gains

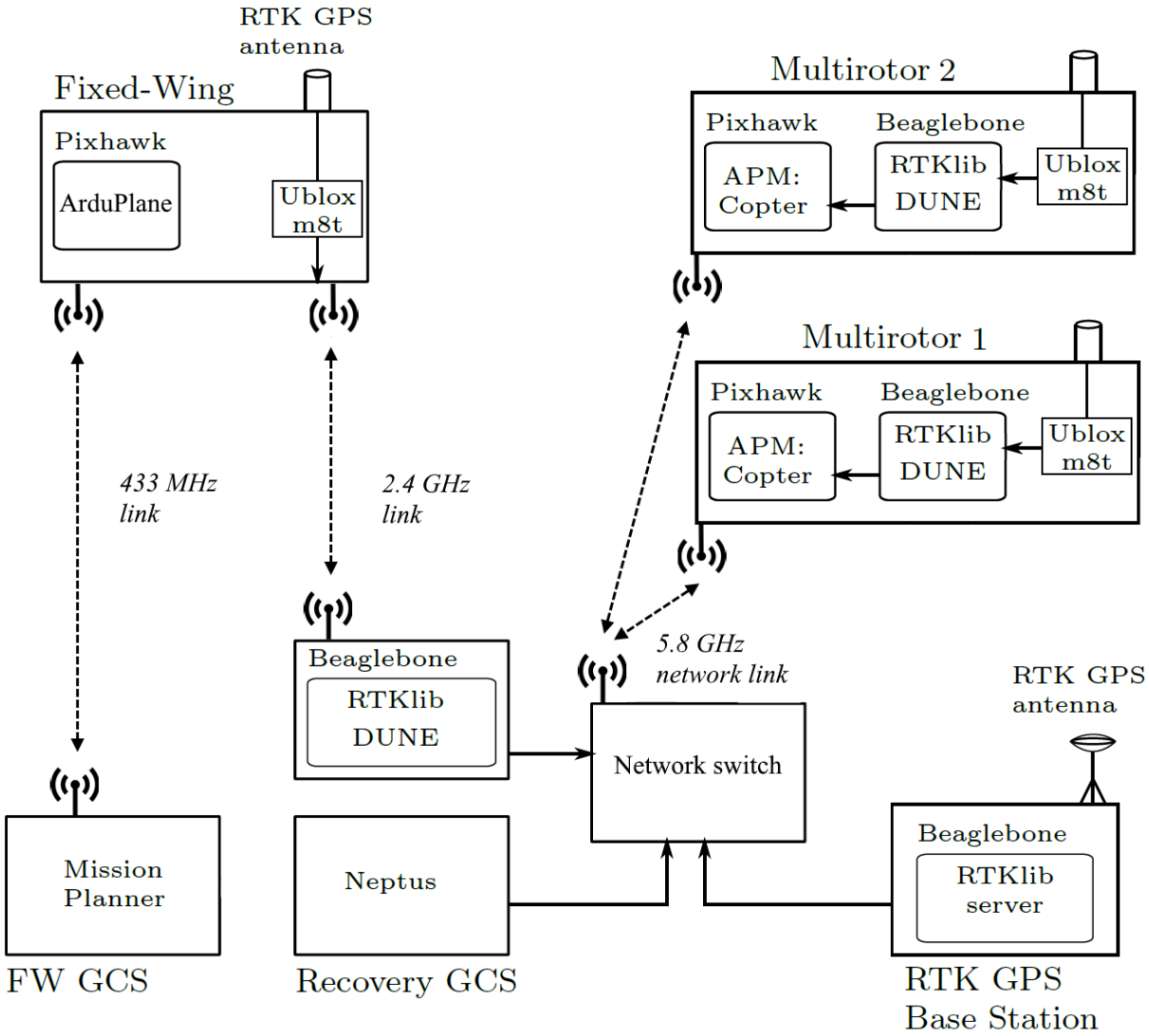

Fig. 6: Overview of the system architecture

TABLE III: Fixed-wing UAV system components

Airframe	Bix3 foam model airplane
Weight	1.4 kg
Low level autopilot	Pixhawk autopilot
Autopilot software	ArduPlane
Companion computer	BeagleBone Black Industrial
CC operating system	Glued
High level control SW	DUNE
Autopilot/CC interface	UART
Autopilot radio link	3DR 433 MHz radio
CC radio link	Microhard PDDL 2.4 GHz link
Navigation system	RTKlib running on CC at 5 Hz
GNSS receiver	Ublox M8T
GNSS antenna	Harxon helical antenna

TABLE IV: Multirotor system components

Airframe	Hexacopter
Weight	2.5 kg
Low level autopilot	Pixhawk autopilot
Autopilot software	APM:Copter
Companion computer	BeagleBone Black Industrial
CC operating system	Glued
High level control SW	DUNE
Autopilot/CC interface	UART
Autopilot radio link	3DR 433 MHz radio
CC radio link	Ubiquity Rocket M5, 5.8 GHz, AirMAX
Navigation system	RTKlib running on CC at 10 Hz
GNSS receiver	Ublox M8T
GNSS antenna	Harxon helical antenna

Fig. 7: The pod used to hold the hook and catch line. The pod is mounted on the fixed-wing airframe with glass fibre reinforced tape. On the line hanging from the pod is a cylinder used to wind the catch line up on. The hook and weight (shown to the right in the hand) is put inside the cylinder when the line is wound up.

- **Manual abort:** Triggered manually by the safety pilot
- **Low battery:** Triggered by battery voltage and remaining capacity
- **Weight of suspended load:** Triggered by the multirotors measuring a line tension of 1.5 kg for more than 0.5 s
- **Communication:** Triggered if any of the vehicles stops sending messages for more than 0.5 s
- **RTK dropout:** Triggered by loss of RTK position for 10 s or loss of RTK base data for 30 s.

These conditions are currently all set up to trigger the same abort behaviour which is that the multirotors will drop the line and go into loiter mode to hold their position. The multirotors will then have to be landed manually by the safety pilots. It is of course possible to implement a more advanced abort logic where the abort behaviour is different depending on the abort condition and maneuver stage. This has not been done in this work as the simple abort logic was considered sufficient for the testing.

D. Operational aspects

During the experimental trials two pilots were involved in the operations. This was made possible by having three different modes of controlling the multirotors:

- **Manual** where each multirotor is controlled by a pilot
- **Formation** where the multirotor formation is controlled by a single pilot
- **Autonomous** where the multirotor formation is flying autonomously controlled by the line-catch controllers

During normal operation, the two multirotors are operated by a single pilot, while a safety pilot is ready to take manual control in case of an emergency. The fixed-wing UAV flies automatically except for in the takeoff where it is under manual control. The operation is as follows:

- Piloted fixed-wing UAV takeoff
- Piloted formation takeoff of the multirotors
- Start of line-catch maneuver. The multirotors and fixed-wing UAV are now flying autonomously
- Release of the catch line from the pod on the fixed-wing UAV before catch
- Autonomous catch of the fixed-wing UAV.
- Piloted formation control of the multirotors when the line-catch maneuver has ended. The fixed-wing UAV is lowered to the ground.
- Optional piloted formation landing of the multirotors by a single pilot or manual landing of the multirotors by both pilots

Pictures of the different stages of the recovery are shown in Figures 8 and 9. Figure 8(a) shows the moment just before the catch and Figure 8(b) shows the moment that the catch line hooks onto the multirotor line. All vehicles are flying autonomously during this stage. Figure 9(a) shows the moment after the catch when the multirotors are at a standstill. At this moment the multirotor formation goes from flying autonomously to being piloted. Figure 9(b) shows the moment when the fixed wing UAV is lowered to the ground by a pilot controlling the multirotor formation.

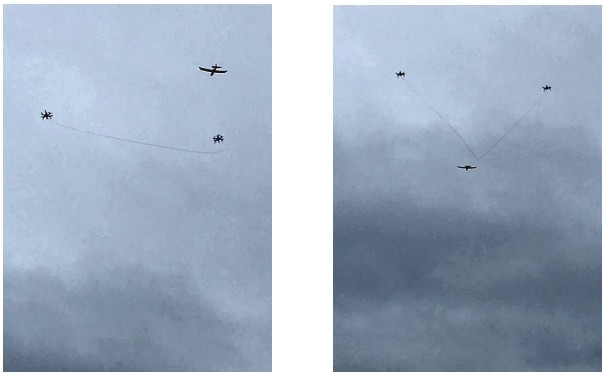

(a) Before catch (b) At catch

Fig. 8: Pictures from the experiments. The first figure shows a moment just before the catch. The second picture shows the moment of the catch. Notice that the hook from the catch line is attached to the multirotor line but the fixed-wing UAV is still flying. Brightness, contrast and sharpness of the pictures is edited to enhance visibility of the line

(a) After catch (b) Fixed-wing on ground

Fig. 9: Pictures from the experiments. The figures show the multirotors carrying the fixed-wing UAV after catch and at the moment the fixed-wing UAV is lowered to the ground. Brightness, contrast and sharpness of the pictures is edited to enhance visibility of the line

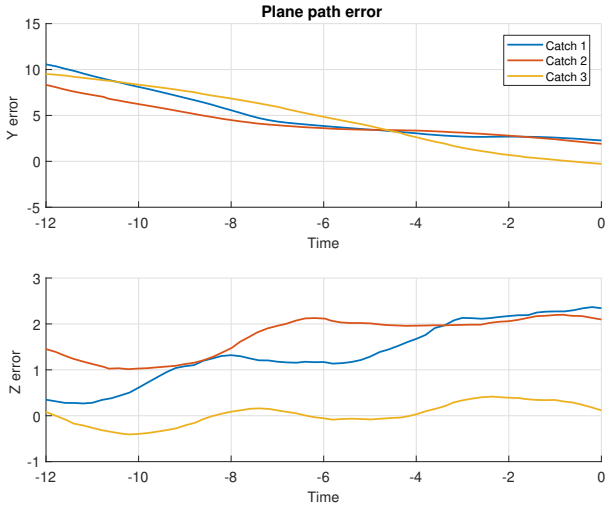

Fig. 10: Fixed-wing UAV path error in y and z direction in the cross track plane. The unit is meters, and zero on the time axis is when the fixed-wing UAV passes the multirotor formation.

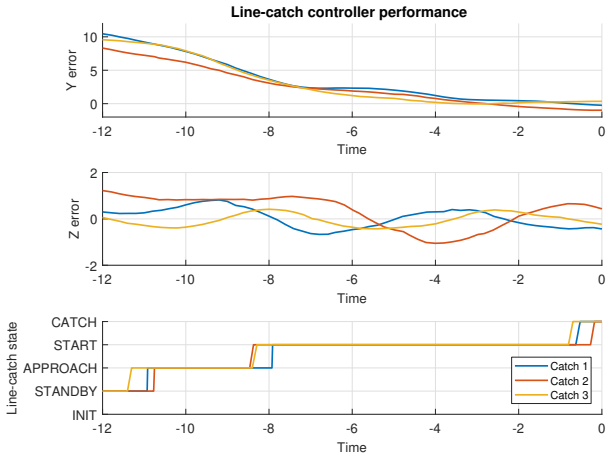

Fig. 11: Multirotor formation controller performance in the cross track plane for the catches. The unit is meters, and zero on the time axis is when the fixed-wing UAV passes the multirotor formation.

V. Results

The results that will be presented here are from 17 test runs and 3 catches. The test runs were performed without lines. The purpose of the test runs were to test different height offsets between the multirotors and the fixed-wing UAV while verifying that the controllers were tuned well enough to enable a catch.

The path error for the fixed-wing UAV is shown in Figure 10 in y and z coordinates of the cross track plane. The figure shows the path error for the three catches. The plot shows that there is a large cross track error at 12 seconds before the catch and that it gradually decreases up until the moment of the catch. The reason for this is a very relaxed tuning of the path controller on the fixed-wing causing it to overshoot the path after a turn.

The performance of the multirotor formation controller in the cross track plane is shown for the catches in Figure 11. Zero on the time scale is at the moment when the fixed-wing UAV passes the multirotors. The initial high error in y is due to the fixed-wing UAV being off the desired path. During the APPROACH phase, the error is decreasing rapidly as the multirotor formation controller is activated. From approximately 3 seconds before the catch the mean of the error for the three catches is close to zero. The error in the z-direction is close to zero for all three catches. The oscillations in the error is due to oscillations in the height of the fixed-wing.

The performance of the line-catch controller over all the test runs is shown in Figure 12 where the distance between the fixed-wing UAV and the multirotor centroid is shown at the moment the fixed-wing UAV passes the multirotors. The maximum distance between the fixed-wing and the multirotor formation was 1.22 m and the mean distance was 0.82 m. The mean of all the points is at $(-0.07, -0.25)$ in the cross track plane. This performance shows that the controllers are

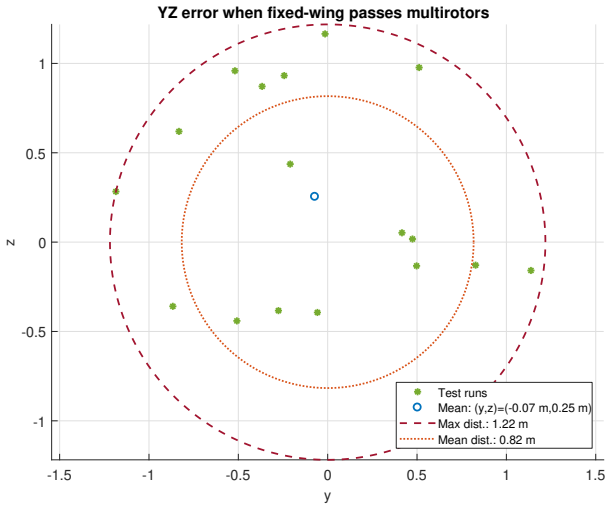

Fig. 12: Distance between fixed-wing UAV and formation centroid when the fixed-wing UAV passes the multirotors for the 17 test runs. The mean point is marked in the figure along with the mean distance from the origin and the maximum distance from the origin.

not very aggressively tuned. The system has been tuned for smooth operations rather than high performance tracking. The reason for this is that the margins for missing the line-catch are rather large and high performance tracking is therefore not needed.

A. Line simulation

In order to gain some more insights from the catches, the lines from the fixed-wing and multirotors have been simulated using the data from the tests. This was done in order to find the margins of missing the catch. The two lines that have been modelled are the catch line suspended from the fixed-wing UAV and the multirotor line suspended between the multirotors. The lines are simulated to get the steady state solution with the assumption of a constant air speed.

1) Multirotor line: The multirotor line has been modelled as a catenary in a standard y-z coordinate system where y is the horizontal axis and z is the vertical axis, [25]:

$$f_{ml}(y) = a\cosh\left(\frac{y}{a}\right) \tag{30}$$

where a is a scaling parameter for the curve. When taking into account the height difference of the multirotors, $h = z_2 - z_1$, the parameters of the catenary are found by solving:

$$w = y_2 - y_1 \tag{31}$$

$$l_{ml} = a\sinh\left(\frac{w}{2a}\right) - a\sinh\left(\frac{-w}{2a}\right) \tag{32}$$

$$h = a\cosh\left(\frac{y_2}{a}\right) - a\cosh\left(\frac{y_1}{a}\right) \tag{33}$$

where y_1 and y_2 are the horizontal positions of the multirotors in the catenary frame, w is the horizontal distance between the multirotors, l_{ml} is the length of the multirotor line, and h is the height difference of the multirotors. The unknown parameters are y_1, y_2 and a and the equations are solved numerically. The effect of the wind drag on the catenary curve is adjusted for by solving the steady state angle of a free hanging cylinder in an air flow in the NED frame:

$$\alpha = \tan^{-1}\left(-\frac{F_z}{F_y}\right) \tag{34}$$

$$F_y = -\sin(\alpha)C_d\frac{1}{2}\rho(\sin(\alpha)\boldsymbol{v}^p_{c,1})^2 d_{ml} \tag{35}$$

$$F_z = mg - \cos(\alpha)C_d\frac{1}{2}\rho(\sin(\alpha)\boldsymbol{v}^p_{c,1})^2 d_{ml} \tag{36}$$

where α is the angle of the line with the horizontal y-axis, F_y and F_z are the forces in the y and z direction respectively, C_d is the drag coefficient of a cylinder, ρ is the density of air, $\boldsymbol{v}^p_{c,1}$ is the airspeed of the multirotor formation in the forward direction, and d_{ml} is the diameter of the multirotor line. The forces F_y and F_z are the unknown parameters. The solution of these equations are used to adjust the catenary for wind drag. The adjusted catenary projected in the multirotor formation cross track yz plane is:

$$z_{cat} = -\sin(\alpha)\left(f_{ml}(y) - \max(f_{ml}(y)) + \frac{h}{2}\right) - z_{off}. \tag{37}$$

2) Catch line: The catch line hanging from the fixed-wing UAV is equipped with a weight at the bottom and a hook at a short distance above the weight. With a low weight of the end-mass/hook, we cannot assume that the line is straight. It is therefore modelled using multiple straight-line segments. The equations used for simulating the ith segment of the line are:

$$\alpha = \tan^{-1}\left(-\frac{F_{z,i-1}}{F_{x,i-1}}\right) \tag{38}$$

$$F_{x,i} = -\sin(\alpha)C_d\frac{1}{2}\rho(\sin(\alpha)\boldsymbol{v}^p_{fw,1})^2 d_{cl} l_i + F_{x,i-1} \tag{39}$$

$$F_{z,i} = m_i g - \cos(\alpha)C_d\frac{1}{2}\rho(\sin(\alpha)\boldsymbol{v}^p_{fw,1})^2 d_{cl} l_i + F_{z,i-1} \tag{40}$$

where, C_d is the drag of the catch line, d_{cl} is the diameter of the catch line, l_i is the length of the ith line segment, m_i is the mass of the ith line segment and $\boldsymbol{v}_{fw,1}$ is the air speed of the fixed-wing in the along track direction. The weight at the bottom of the line is simulated as a sphere:

$$F_{x,0} = C_{ds}\frac{1}{2}\rho(\boldsymbol{v}^p_{fw,1})^2\pi r_w^2 \tag{41}$$

$$F_{z,0} = m_w g \tag{42}$$

where C_{ds} is the drag coefficient for a sphere, r_w is the radius of the catch line and m_w is the weight of the catch line. The simulation is solved by starting at the weight at the bottom and then solving upwards for each of the line segments. The forces of the hook are calculated as if it was a sphere. We note that these formulas are also useful to adjust the vertical offset z_{off} when the geometry of the lines changes if a different airspeed is required during recovery. The simulated catch line and multi-rotor line are illustrated in the example in Figure 13.

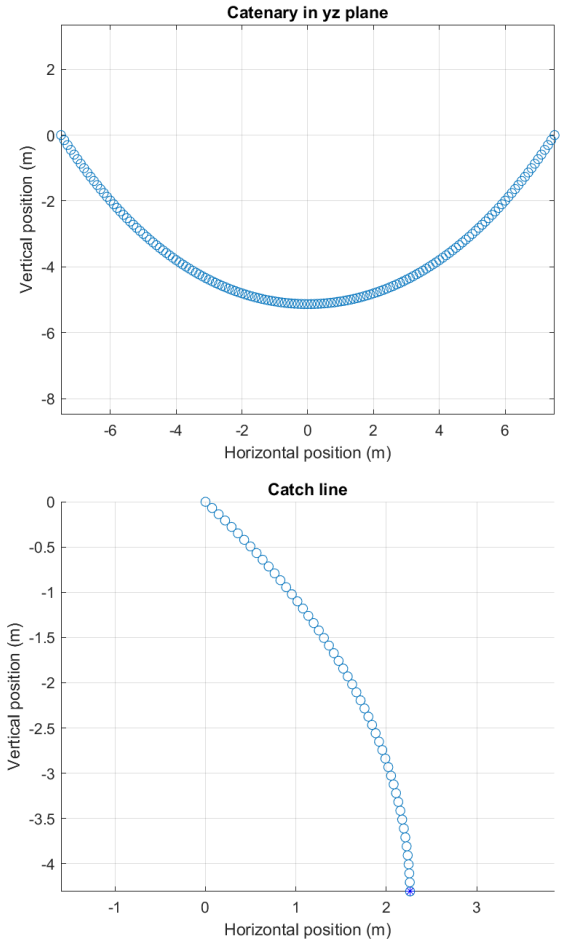

Fig. 13: Example of simulated multi-rotor line (upper) and catch line (lower). The circles indicate the discretization points of the catch line simulation.

B. Catch margins

A successful catch depends on the relative position of the multirotor line and the catch line when they intercept at the time the fixed-wing UAV passes the multirotor formation. With given airspeeds of the vehicles, this leads to requirements on the relative position of the fixed-wing UAV relative to the multirotor formation centroid.

A successful catch requires that this relative position belongs to the catch set, which is illustrted in Figure 14. The lower boundary of the catch set is equal to the position of the multirotor line, while the upper bounary is defined by the same multirotor line shifted upwards a distance that is equal to the vertical length of the catch line. In addition, the upper bounary is capped at the position of the multirotors as it is not desirable to have the fixed-wing flying above the multirotors due to the risk of entangling the catch line in the propellers of the multirotors. The catch margin is well-defined and exists if the relative position of the fixed-wing UAV is within the boundaries of the catch set. The catch margin is then defined as the distance from the fixed-wing UAV's relative position to the closest point on the boundary of the catch set. This means that it is generally desirable with highest possible catch

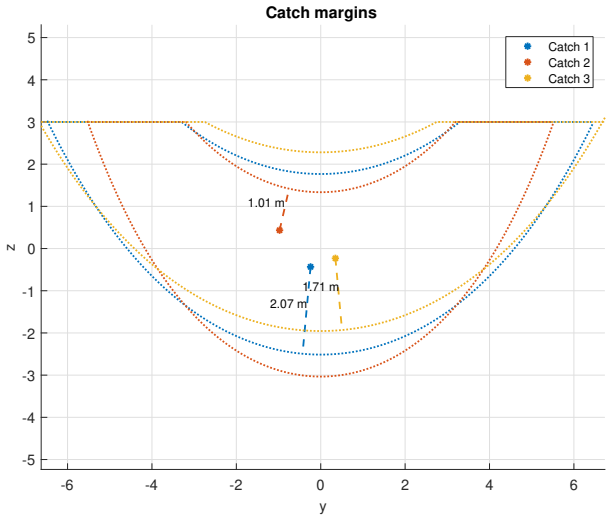

Fig. 14: Catch set and margins for missing the catch for each of the three catches. The smallest margin and direction are marked.

TABLE V: Width and height of catch area at origin of cross track plane

Catch number	Height	Width	Max margin
Catch 1	4.28 m	8.42 m	2.14 m
Catch 2	4.34 m	8.82 m	2.17 m
Catch 3	4.23 m	8.33 m	2.12 m

margins, and a non-existing catch margin implies that the catch is missed, which is a recovery failure.

The margins for the three catches are shown in Figure 14. Since the location of the lines are not measured during the experiments, the lines are instead simulated at the time the fixed-wing UAV passes the multirotor formation in order to find the margins for missing the catch. It can be seen from the figure that the smallest margin for the three catches is 1.01 meter and the largest is 2.07 meters. The width and height of the catch area at the origin of the cross track plane is shown in Table V along with the maximum possible margin. The maximum possible margin is between 2.1-2.2 meters for the three catches. If the margins shown in Figure 14 are compared to this, it is clear that the margins seen in the three catches are relatively large.

In Figure 15 the catch margins are shown in the APPROACH and START phases for the three catches. The margins shown in the figure are calculated by simulating the lines at each point in time and the margin is shown as negative if the fixed-wing UAV would have missed. The figure shows that the catch margins are positive during the whole START phase with 0.4 m being the smallest value. This shows that even though the tuning of the controllers is relatively relaxed, the multirotors are able to track the fixed-wing UAV's path well enough to keep it within the catch margins.

C. Multirotor load

The load on the multirotors from the multirotor line is shown in Figure 16 for the three catches. The figure shows

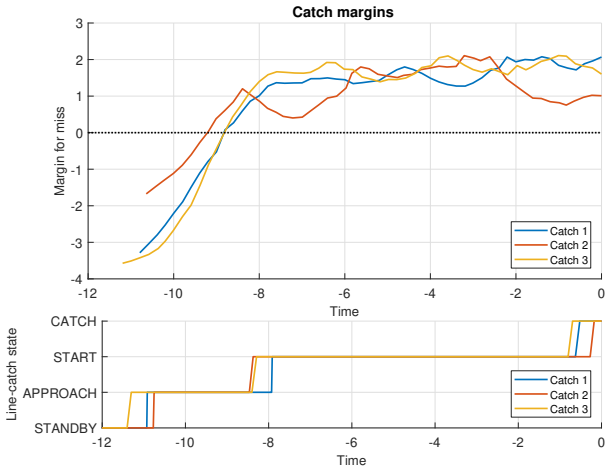

Fig. 15: Margins for missing the catch (in meters) in the APPROACH and START phases.

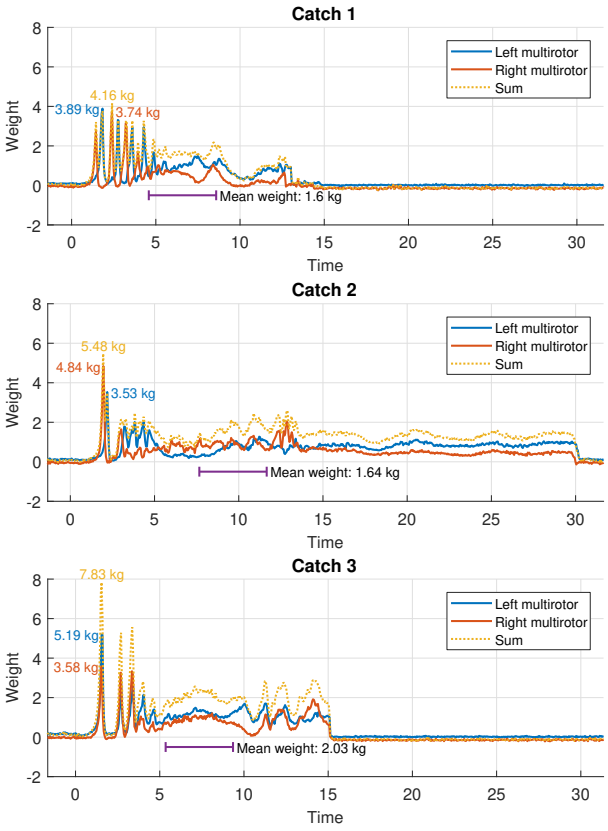

Fig. 16: Weight measured on the multirotor line by each of the multirotors and the total weight on the line. Peak weight and mean weight after the catch is shown in the plot.

the mean tension after the catch. The window which the mean tension is calculated in is chosen as the 4 seconds after the catch with the least accelerations by the multirotor formation. The mean tension is higher at the third catch which is due to accelerations of the multirotors. The maximum tension shown in the figure for the catches shows that each of the multirotors are subject to a peak tension between 3.5-5.2 kg. Dividing this by the mass of the fixed-wing and catch lines which is 1.6 kg, we find that a single multirotor should be able to withstand a peak weight of 3.25 times the weight of the fixed-wing for a short period of time. All the peaks last for less than a second and the oscillations resulting in the tension peaks are successfully dampened by the controllers 5 seconds after the catch.

VI. Discussion and Future Work

The most obvious way to improve the catch margins would be to use a longer catch line on the fixed-wing and a longer line between the multirotors. However, as long as the multirotor formation is at some point operated by a pilot, the formation needs to be narrow enough for the pilot to keep both in view while being a reasonable distance from the formation. When the flight of the formation is automated, the length of the lines between the multirotors and from the fixed-wing UAV can be increased considerably. The challenges in doing this would mostly be of practical character as the new platforms needed to be prepared for the tests but would also include tuning some of the parameter values such as the desired speed of the multirotors during the recovery.

In order to improve the catch margins with the current multirotor line, the fixed wing UAV could be equipped with a longer catch line and the vertical offset z_{off} between the formation middle and the centroid could be decreased. If the offset z_{off} is decreased to 1 m the fixed-wing UAV would be 1 m below the multirotor formation middle point at the time of catch, assuming perfect controllers. Using the line simulations from the three catches, this would mean a maximum horizontal margin of 5-6 m and a maximum vertical margin of 4-5 m if a 10 m catch line was used on the fixed-wing UAV. In the best case, this is twice as much as the maximum margins shown in Table V. The cost of these better margins are a slightly higher risk of collision between the fixed-wing UAV and the multirotors as the vertical distance is less. However, from Figure 11 and 14 we can see that the tracking error is less than 1.2 m when the fixed-wing UAV passed the multirotors in 95% of the passes when combining the test runs and the catches. The risk of a collision of the fixed-wing UAV and the multirotors would therefore be minimal even if the vertical offset was 1 m.

It was suggested that using longer lines between the multirotors and from the fixed-wing UAV could increase the margins and that the margins could be improved with the existing lines by moving decreasing the distance between the multirotor formation and the fixed-wing. A challenge with longer lines is increased weight and drag, and an important direction for future research is to consider line materials and analysing and predicting in more detail the resulting line geometry and dynamics using simulation tools.

Since the concept of a virtual runway offers flexibility with respect to its location and orientation, the virtual runway is recommended to be aligned with the mean wind direction such that the fixed-wing UAV follows a path straight into the wind. Moreover, since the multirotors and the fixed-wing UAV are exposed to the same mean wind velocity, the performance during the recovery is not significantly influenced

by the mean wind velocity and direction, assuming the virtual runway is aligned with the mean wind direction. However, wind gusts and turbulence will have significant influence on control accuracy of both the fixed-wing UAV and the multi-rotors, and they may also influence the orientation and motion of the lines. The motion of the ship relative to the wind is also a factor that influences the energy required to deploy the multi-rotors to the virtual runway, as well as the energy needed recovering the multirotors with the catched fixed-wing UAV back to the ship. The energy budget of the multirotor UAVs must be sufficient for this to be feasible. In summary, it is clear that the operational limitations are set by wind gusts, turbulence as well as the ship motion and mean wind velocity through their influence on the range and endurance of the multirotor UAVs. The operational limitations of the system are not analyzed in this paper, and is suggested as important topics for future work.

The different GNSS receivers need to have the same reference for altitude, and we note that sufficient altitude accuracy is generally not achieved with GNSS without differential corrections. Hence, the system relies on moving-baseline RTK GNSS, and an improvement would be to be able to use this recovery concept also when RTK GNSS drops out for shorter period of time using inertial navigation and possibly aiding by local navigation systems such as ultra wideband localization, [26]. Moreover, if longer lines are used between the multirotors and from the fixed-wing UAV, the catch margins could be higher and the requirement for navigation precision would be less and using a less accurate navigation system should therefore be possible.

Future work could also be to automate landing and takeoff of the multirotor formation such that no operator would be needed at all in order to make the method fully autonomous. This could be based on existing methods such as [27].

VII. Conclusion

This article presents a novel method for recovery of a fixed-wing UAV using two multirotor UAVs with a line suspended between them. The concept of the recovery was described along with the control system used for testing the concept experimentally. The experimental results were analysed and it was found that for 17 test runs the maximum distance between the fixed-wing UAV and the multirotor formation centroid was 1.22 m at the moment when the fixed-wing UAV passes the multirotors. Three catches were performed where the margins for miss at the moment of catch were 1.01 m, 1.71 m and 2.07 m. For all three catches, the margins for a miss were always positive (meaning the fixed-wing UAV would be caught) from a few seconds after the activation of the controllers until the catch happened.

Acknowledgement

The authors would like to thank Kristian Klausen and UAV operators Pål Kvaløy, NTNU; Lars Semb, Maritime Robotics and Carl Erik Stephansen, Maritime Robotics for their invaluable aid in preparing and performing the experiments.

This project has received funding from the European Union's Horizon 2020 research and innovation programme under the Marie Sklodowska-Curie grant agreement No 642153, and the Research Council of Norway through grants 223254, 269480 and 282427.

References

[1] A. Gautam, P. B. Sujit, and S. Saripalli, "A survey of autonomous landing techniques for uavs," in *2014 International Conference on Unmanned Aircraft Systems (ICUAS)*, May 2014, pp. 1210–1218.

[2] B. Yuksek, A. Vuruskan, U. Ozdemir, M. A. Yukselen, and G. a. Inalhan, "Transition flight modeling of a fixed-wing VTOL UAV," *J. Intelligent and Robotic Systems*, vol. 84, pp. 83 – 105, 2016.

[3] A. S. Saeed, A. B. Younes, S. Islam, J. Dias, L. Seneviratne, and G. Cai, "A review on the platform design, dynamic modeling and control of hybrid uavs," in *Proc. Int Conf Unmanned Aircraft Systems*, 2015.

[4] M. Tyan, N. V. Nguyen, S. Kim, and J.-W. Lee, "Comprehensive preliminary sizing/resizing method for a fixed wing – VTOl electric UAV," *Aerospace Science and Technology*, vol. 71, pp. 30–41, 2017.

[5] M. Laiacker, K. Kondak, M. Schwarzbach, and T. Muskardin, "Vision aided automatic landing system for fixed wing uav," in *2013 IEEE/RSJ International Conference on Intelligent Robots and Systems*, Nov 2013, pp. 2971–2976.

[6] S. Thurrowgood, R. J. D. Moore, D. Soccol, M. Knight, and M. V. Srinivasan, "A biologically inspired, vision-based guidance system for automatic landing of a fixed-wing aircraft," *J. Field Robot.*, vol. 31, no. 4, pp. 699–727, Jul. 2014. [Online]. Available: http://dx.doi.org/10.1002/rob.21527

[7] H. J. Kim, M. Kim, H. Lim, C. Park, S. Yoon, D. Lee, H. Choi, G. Oh, J. Park, and Y. Kim, "Fully autonomous vision-based net-recovery landing system for a fixed-wing uav," *IEEE/ASME Transactions on Mechatronics*, vol. 18, no. 4, pp. 1320–1333, Aug 2013.

[8] S. Huh and D. H. Shim, "A vision-based landing system for small unmanned aerial vehicles using an airbag," *Control Engineering Practice*, vol. 18, no. 7, pp. 812 – 823, 2010, special Issue on Aerial Robotics. [Online]. Available: http://www.sciencedirect.com/science/article/pii/S0967066110001206

[9] T. Muskardin, G. Balmer, L. Persson, S. Wlach, M. Laiacker, A. Ollero, and K. Kondak, "A novel landing system to increase payload capacity and operational availability of high altitude long endurance uav," in *2016 International Conference on Unmanned Aircraft Systems (ICUAS)*, June 2016, pp. 495–504.

[10] R. Skulstad, C. Syversen, M. Merz, N. Sokolova, T. Fossen, and T. Johansen, "Autonomous net recovery of fixed- wing uav with single-frequency carrier-phase differential gnss," *IEEE Aerospace and Electronic Systems Magazine*, vol. 30, no. 5, pp. 18–27, May 2015.

[11] S. H. Mathisen, K. Gryte, T. A. Johansen, and T. I. Fossen, "Non-linear model predictive control for longitudinal and lateral guidance of a small fixed-wing uav in precision deep stall landing," in *AIAA Guidance, Navigation, and Control Conference, San Diego*, 2016, p. 0512.

[12] Zipline, "How zipline works," 2019. [Online]. Available: http://www.flyzipline.com/service/

[13] Insitu, "Skyhook," 2019. [Online]. Available: https://www.insitu.com/images/uploads/pdfs/Skyhook_Universal_ProductCard_PR041615.pdf

[14] DARPA, "Sidearm prototype catches full-size unmanned aerial system flying at full speed," 2017. [Online]. Available: https://www.darpa.mil/news-events/2017-02-06

[15] J. W. Nichols, L. Sun, R. W. Beard, and T. McLain, "Aerial rendezvous of small unmanned aircraft using a passive towed cable system," *J. Guidance, Dynamics and Control*, vol. 37, 2014.

[16] K. Klausen, J. B. Moe, J. C. van den Hoorn, A. Gomola, T. I. Fossen, and T. A. Johansen, "Coordinated control concept for recovery of a fixed-wing uav on a ship using a net carried by multirotor uavs," in *2016 International Conference on Unmanned Aircraft Systems (ICUAS)*, June 2016, pp. 964–973.

[17] K. Klausen, T. I. Fossen, and T. A. Johansen, "Autonomous recovery of a fixed-wing uav using a net suspended by two multirotor uavs," *Journal of Field Robotics*, vol. 35, no. 5, pp. 717–731, 2017.

[18] R. Mahony, V. Kumar, and P. Corke, "Multirotor aerial vehicles: Modeling, estimation, and control of quadrotor," *IEEE Robotics Automation Magazine*, vol. 19, no. 3, pp. 20–32, Sep. 2012.

[19] H. Bai, M. Arcak, and J. T. Wen, *Cooperative control design. A systematic, passivity-based approach.* Springer, 2011, vol. 89.

[20] K. Klausen, C. Meissen, T. I. Fossen, M. Arcak, and T. A. Johansen, "Cooperative control for multirotors transporting an unknown suspended load under environmental disturbances," *IEEE Transactions on Control Systems Technology*, vol. 28, pp. 653–660, 2020.
[21] J. Pinto, P. S. Dias, R. Martins, J. Fortuna, E. Marques, and J. Sousa, "The lsts toolchain for networked vehicle systems," in *2013 MTS/IEEE OCEANS - Bergen*, June 2013, pp. 1–9.
[22] T. Takasu and A. Yasuda, "Development of the low-cost rtk-gps receiver with an open source program package rtklib," *International Symposium on GPS/GNSS*, 01 2009.
[23] A. P. Zolich, T. A. Johansen, K. P. Cisek, and K. Klausen, "Unmanned aerial system architecture for maritime missions. design and hardware description," in *Workshop on Research, Education and Development of Unmanned Aerial Systems (RED-UAS)*, 2015.
[24] N. A. Haukanes, "Fixed-wing autolanding systems: System design for line-catch release mechanism," MSC thesis, Norwegian University of Science and Technology, Trondheim, Tech. Rep., 2017.
[25] J. Stewart, *Essential Calculus: Early Transcendentals*. Brooks/Cole, 2010.
[26] K. Gryte, J. M. Hansen, T. A. Johansen, and T. I. Fossen, "Robust navigation of uav using inertial sensors aided by uwb and rtk gps," in *AIAA Guidance, Navigation, and Control Conference, Grapevine, TX*, 2017.
[27] T. S. Richardson, C. G. Jones, A. Likhoded, E. Sparks, A. Jordan, I. Cowling, and S. Willcox, "Automated vision-based recovery of a rotary wing unmanned aerial vehicle onto a moving platform," *Journal of Field Robotics*, vol. 30, no. 5, pp. 667–684, 2013.

BIOGRAPHIES

Mads Bornebusch received the M.Sc. degree in Electrical Engineering from the Technical University of Denmark (DTU) in 2017. His research at the Department of Engineering Cybernetics, Norwegian University of Science and Technology, was on guidance, navigation and control of formations of fixed wing and multirotor unmanned aerial vehicles with application to landing of fixed wing UAVs.

Tor Arne Johansen received the MSc degree in 1989 and the PhD degree in 1994, both in electrical and computer engineering, from the Norwegian University of Science and Technology, Trondheim, Norway. From 1995 to 1997, he worked at SINTEF as a researcher before he was appointed Associated Professor at the Norwegian University of Science and Technology in Trondheim in 1997 and Professor in 2001. He has published several hundred articles in the areas of control, estimation and optimization with applications in the marine, aerospace, automotive, biomedical and process industries. In 2002 Johansen co-founded the company Marine Cybernetics AS where he was Vice President until 2008. Prof. Johansen received the 2006 Arch T. Colwell Merit Award of the SAE, and is currently a principal researcher within the Center of Excellence on Autonomous Marine Operations and Systems (NTNU-AMOS) and director of the Unmanned Aerial Vehicle Laboratory at NTNU and the SmallSat Laboratory at NTNU. He recently co-founded the spin-off companies Scout Drone Inspection, UBIQ Aerospace and Zeabuz.